

## High Structural Stability and Adsorption Capacity of Zn/Al-Biochar and Cu/Al-Biochar Toward Adsorption of Cr(VI)

Neza Rahayu Palapa<sup>1</sup>, Tarmizi Taher<sup>2,4</sup>, Patimah Mega Syah Bahar Nur Siregar<sup>3</sup>, Normah<sup>3</sup>, Novie Juleanti<sup>3</sup>, Alfian Wijaya<sup>3</sup>, Arini Fousty Badri<sup>1</sup>, Aldes Lesbani<sup>1,4\*</sup>

<sup>1</sup> Graduate School, Faculty of Mathematics and Natural Sciences, Universitas Sriwijaya, Jl. Palembang-Prabumulih, Km. 32, Ogan Ilir, South Sumatera, Indonesia

<sup>2</sup> Department of Environmental Engineering, Institut Teknologi Sumatera, Jalan Terusan Ryacudu, Way Hui, Kecamatan Jati Agung, Lampung Selatan 35365, Indonesia

<sup>3</sup> Department of Chemistry, Faculty of Mathematics and Natural Sciences, Universitas Sriwijaya, Jl. Padang Selasa No. 524 Ilir Barat 1, Palembang-South Sumatera, Indonesia

<sup>4</sup> Research Center of Inorganic Materials and Complexes, Faculty of Mathematics and Natural Sciences, Universitas Sriwijaya, Jl. Padang Selasa Bukit Besar Palembang 30139, South Sumatera, Indonesia

\* Corresponding author's email: [aldeslesbani@pps.unsri.ac.id](mailto:aldeslesbani@pps.unsri.ac.id)

### ABSTRACT

Layered double hydroxide (LDH) Zn/Al and Cu/Al was synthesized by using the coprecipitation method under base condition at pH 10 following with formation of composites based on biochar (BC) to form Zn/Al-BC and Cu/Al-BC. The materials were characterized by XRD, FTIR, BET, and thermal analyses. Furthermore, materials was applied as adsorbent of Cr(VI) on aqueous solution. The performance of composites as adsorbent was evaluated by reusability of adsorbent toward Cr(VI) adsorption process. The results showed that Cu/Al-BC and Zn/Al-BC can reuse the re-adsorption process with the adsorption ability of more than 60%. The adsorption capacity of Cu/Al-BC and Zn/Al-BC was higher than that of starting materials and up to 384.615 mg/g for Cu/Al-BC and 666.667 mg/g for Zn/Al-BC. Both composites showed the potential adsorbents to remove Cr(VI) from aqueous solution.

**Keywords:** layered double hydroxide, chromium, adsorption, reusability

### INTRODUCTION

Heavy metal ions in aquatic systems are major inorganic pollutants in the environment [Nagar et al., 2018]. Heavy metal ions in wastewater have a stable form and are non-degradable [Wu et al., 2020; Rahman, 2020]. Moreover, heavy metal ions can accumulate on biota and create high stability in a human body [Kahlon et al., 2018]. The effect of heavy metal ions on a human body ranges from headache to vomiting and can be lethal due to the accumulation process; thus, the removal of heavy metal ions from wastewater is vital. Chromium is one of the important toxic heavy metal ions. Chromium has several oxidation states but chromium (+6) is the most toxic species [Forghani et al., 2020]. Chromium can

be produced by several activities, ranging from home to industrial applications such as photo film [Saha et al., 2011], electroplating [Hosseinkhani et al., 2020], painting [Begum et al., 2019], and also agricultural agents [Itankar and Patil, 2014]. The removal of chromium(VI) from an aqueous solution was conducted by many researchers using such methods as coagulation [Golder et al., 2007], membrane filtration [Sun et al., 2013], reduction [Altun and Kar, 2016], and also adsorption [Wang et al., 2020]. Among these methods, adsorption is suitable way to remove chromium ions by fast [Sun et al., 2013] and easy processes [Kaykhani et al., 2018].

The successful adsorption process is very dependent on the adsorbent properties. Adsorbents can be classified as organic [Ali et al., 2012]

and inorganic adsorbents [Miguel et al., 2008]. Organic adsorbents such as chitin, chitosan [Semeraro et al., 2017], cellulose [Gasemloo et al., 2019], and algae [de Bittencourt et al., 2020] have limitation due to the reusability of adsorbent. Although these adsorbents have various active sites, the reusability properties of these materials are very limited. On the other hand, inorganic materials have such advantages as stability at high temperature, structural stability, and also reusability of materials. The examples of these adsorbents include zeolite [Zhang et al., 2020], bentonite [Castro-Castro et al., 2020], montmorillonite [Sivamani and Leena, 2009], metal oxide [Kaur et al., 2021], and also layered double hydroxide [Shan et al., 2015].

Layered double hydroxide (LDH) is inorganic material consisting of divalent and trivalent metal ions with general formula  $[M^{2+}_{1-x}M^{3+}_x(OH)_2]^{x+}(A^{n-})_{x/n} \cdot nH_2O$ , where  $M^{2+}$  is divalent ions,  $M^{3+}$  is trivalent ions, and  $A^{n-}$  is an anion on interlayer with  $n$  valence [Bouteraa et al., 2020]. Divalent and trivalent ions of LDH can be exchangeable with wide range metals on periodic table [Mir et al., 2020]. The most important properties of LDH is the modification of these materials in various ways to obtain LDH with specific application.

The use of Zn/Al LDH as an adsorbent of Cr(VI) was studied by [Cocheci et al., 2010]. Zn-Al LDH with carbonate on interlayer space and contains small impurities. Cr(VI) was an adsorbent within the cavities of metal hydroxide at the edge of the brucite layer. The removal of Cr(VI) from an aqueous solution was also conducted by Mg/Al LDH [Otgongjargal et al., 2017]. This Mg/Al was thermally treated after coprecipitation to improve the Cr(VI) adsorption with the adsorption capacity of 88.07 mg/g. All these results showed that the use of pristine LDH has low adsorption capacity for Cr(VI) removal. Modification of LDH to improve the adsorption capacity of Cr(VI) was reported by several researchers. Sand coated Mg/Al LDH was prepared by coprecipitation and in-situ process. The Cr(VI) adsorption by sand coated Mg/Al LDH follows pseudo second-order kinetic model and has high Langmuir adsorption capacity [Gao et al., 2018]. On the other hand, Mg/Al LDH was modified by biochar following with intercalation by ethylenediaminetetraacetic acid on interlayer space of LDH as adsorbent of Cr(VI) from aqueous solution. Although the adsorption

capacity was only 38 mg/g but biochar has an important key for the binding of Cr(VI) on adsorbent [Huang et al., 2019]. On the basis of these works, it is intriguing and vital to conduct the modification of LDH to improve the adsorption capacity and mechanism.

In this research, LDH of Cu/Al and Zn/Al with different divalent ions was prepared and modified by biochar (BC) to form composites of Cu/Al-BC and Zn/Al-BC. The high structural stability of composites was expected, which was equal to the increasing surface area properties. The composites of Cu/Al-BC and Zn/Al-BC were used as adsorbents of chromium(VI) from aqueous solution. The first aim of this research was to evaluate the stability of adsorbents toward Cr(VI) re-adsorption process after desorption by ultrasonic system. The second goal was to determine the isotherm and thermodynamic properties of Cr(VI) adsorption on composites and starting materials.

## MATERIALS AND METHODS

### Chemical and instrumentation

Chemicals used in the study were purchased from Merck and Sigma-Aldrich, including as copper(II) nitrate, aluminum(III) nitrate, zinc(II) nitrate, potassium dichromate, and sodium hydroxide. BC was obtained from Bukata Organic® Java Island, Indonesia. BC was produced from Java rice husk by pyrolysis according to [Vieira et al., 2020]. Water was supplied from Research Center of Inorganic Materials and Complexes FMIPA Universitas Sriwijaya, Indonesia after purification using Purite®. The materials were characterized by XRD, FTIR, BET, and thermal analyses. The analysis of powder XRD was performed by means of a Rigaku Miniflex-600 diffractometer. The sample was scanned at 1°/min. IR spectra were obtained by FTIR Shimadzu Prestige-21 using KBr pellet and sample was scanned at 400-4000  $cm^{-1}$ . The BET data was obtained from  $N_2$  adsorption-desorption analysis using a Quantachrome micrometric 2020. Thermal analysis was conducted using a TG-DTA Shimadzu analyzer by  $N_2$  flow. The concentration of Cr(VI) on solution was analyzed with a UV-Vis Bio-Base BK-UV 1800 PC spectrophotometer at 543 nm after complexation by diphenylcarbazide as a ligand.

## Synthesis of Cu/Al and Zn/Al LDHs

Synthesis of Cu/Al and Zn/Al LDHs was conducted by coprecipitation method under base condition at pH 10 as similar procedure by [Palapa et al., 2019]. A solution of copper(II) nitrate and aluminum(III) nitrate with molar ratio 3:1 was mixed with equal volume under constant stirring at room temperature. The pH of reaction was adjusted to 10 by the addition of the sodium hydroxide solution. The reaction was constantly stirred at 80°C for 30 hours to form solid material. A similar procedure was repeated for zinc(II) nitrate and aluminum(III) nitrate. Solid material was filtered, washed with water, and dried at 110°C.

## Preparation of Cu/Al-BC and Zn/Al-BC

A composite of Cu/Al-BC and Zn/Al-BC was prepared by the co-precipitation method [Palapa et al., 2020a]. The solution of  $M^{2+}$  ( $M^{2+} = \text{Cu}$  or  $\text{Zn}$ ) was mixed with aluminum(III) nitrate with molar ratio 3:1 at equal volume. The reaction mixtures were constantly stirred at room temperature, then 3 g of BC was added with vigorous stirring. The solution of sodium hydroxide was added to reach pH 10. The reaction mixtures were constantly stirred for 72 hours to form the Cu/Al-BC and Zn/Al-BC composites. The composites were filtered and washed with water three times. The composites were characterized after dry materials at 110 °C.

## Regenerations studies

Regeneration studies were performed to evaluate the structural stability of composite and pristine materials toward Cr(VI) re-adsorption. The materials were desorbed by ultrasonic system for 30 minutes after the adsorption process, then dried at 110 °C. Re-adsorption was performed by the same adsorbent after the desorption process. Re-adsorption was conducted until five cycles adsorption-desorption of Cr(VI).

## Adsorption experiment

Adsorption of Cr(VI) was conducted by batch system equipped with magnetic bar, and shaker systems [Oktriyanti et al., 2019]. Adsorption was performed by variation of Cr(VI) initial concentrations and adsorption temperatures. The initial concentration of Cr(VI) was adjusted at 10, 20,

30, 40, 50 mg/L and adsorption temperatures at 30, 40, 50, 60°C. The concentration of Cr(VI) on solution was analyzed after complexation of Cr(VI) by diphenylcarbazide to form a [Cr-diphenylcarbazide] complex. The wavelength of analysis was adjusted at 543 nm.

## RESULTS AND DISCUSSION

The XRD powder patterns of Zn/Al LDH, Cu/Al LDH, BC, and composites were presented in (Fig. 1). Main diffraction peaks of layered materials were identified at (003), (006), and (110) at 10-15°, 20-24°, and 60-61° [Palapa et al, 2020; Silaen et al, 2020]. These peaks were assigned as well-known formation of layered materials of LDH. Both Zn/Al and Cu/Al LDHs had high crystallinity materials [Mandal et al., 2013]. The diffraction peak at 30° on Zn/Al LDH was found due to the formation of metal oxide on LDH, which was mixed on the interlayer material [Marques et al., 2020]. The diffraction peak of BC as shown in Figure 1c showed that a broad peak occurred due to high carbon content on BC as organic material. The diffraction at 22.30° (002) was attributed to carbon on BC [Amen et al., 2020]. The composites of Zn/Al-BC and Cu/Al-BC had all diffraction peaks of LDH and BC at 10-15°, 22-24° and also at 60-61°, as shown in Figures 1d and e. Although both Zn/Al-BC and Cu/Al-BC had diffraction of pristine materials but the crystallinity of these composites was a slightly different. Zn/Al-BC had higher crystallinity properties than Cu/Al-BC. This was probably due to involvement of d empty orbital on Cu which can slightly decrease the crystallinity properties in comparison to Zn.

The FTIR spectrum of Zn/Al and Cu/Al LDHs had vibrations at 3448  $\text{cm}^{-1}$  (u O-H stretching), 1635  $\text{cm}^{-1}$  (u O-H bending), 1381  $\text{cm}^{-1}$  (u N-O nitrate stretching), 794  $\text{cm}^{-1}$  (u Al-O) and 462  $\text{cm}^{-1}$  (u Zn-O, Cu-O), as shown in Figures 2a and b [Palapa et al., 2020b]. BC was an organic material; thus, it had vibrations at 3448  $\text{cm}^{-1}$  (u O-H stretching), 2368  $\text{cm}^{-1}$  (u C-H), 1635  $\text{cm}^{-1}$  (u O-H bending), and 1095  $\text{cm}^{-1}$  (u C-O stretching) [Amen et al., 2020]. The composites of Zn/Al-BC and Cu/Al-BC had all vibrations of LDH and BC, as a results of two components were involved in composites.

The  $\text{N}_2$  adsorption-desorption isotherm of composites and starting materials was shown in (Fig. 3). All materials had hysteresis loop because

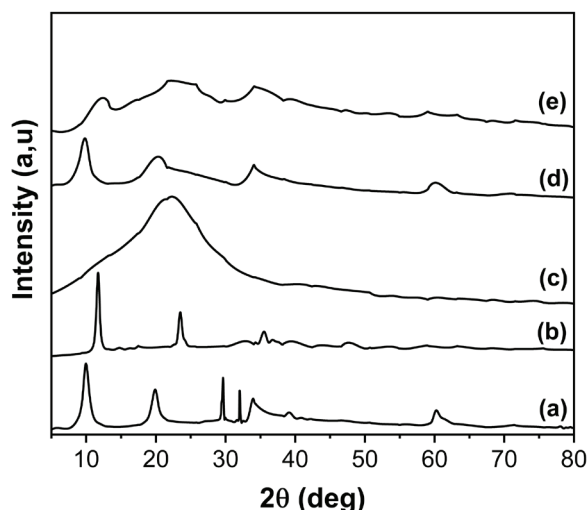


**Figure 1.** XRD powder patterns of Zn/Al LDH (a), Cu/Al LDH (b), BC (c), Zn/Al-BC (d), Cu/Al-BC (e)

adsorption was different from the desorption patterns. The materials had micropores and mesopores sizes, which were mixed with each other on the lattice of composites and starting materials [Moller and Pich, 2017]. The hysteresis loop was largely found on BC, Zn/Al-BC, and Cu/Al-BC probably due to carbon based material involve on inorganic layer of LDH [Palapa et al, 2020b]. The Brunauer-Emmett-Teller (BET) of materials was obtained by calculation of data in (Fig. 3) and the results were presented in (Tab. 1).

Table 1 showed that Cu/Al-BC and Zn/Al-BC had the surface area four-fold and six-fold higher, respectively, than pristine LDH. This was probably due to the high crystallinity of Zn/Al-BC

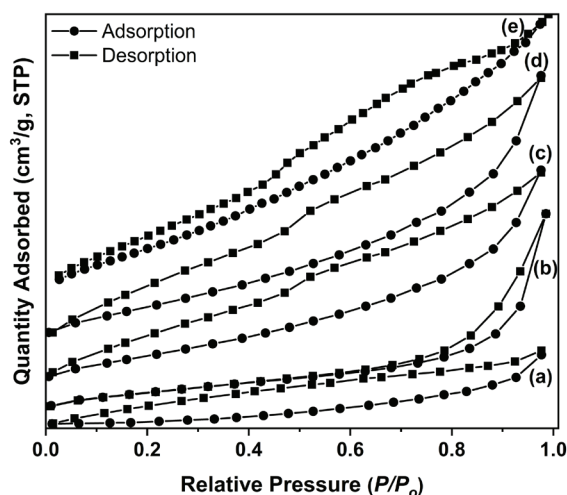


**Figure 3.** Nitrogen adsorption-desorption isotherm of Zn/Al LDH (a), Cu/Al LDH (b), BC (c), Zn/Al-BC (d), Cu/Al-BC (e)

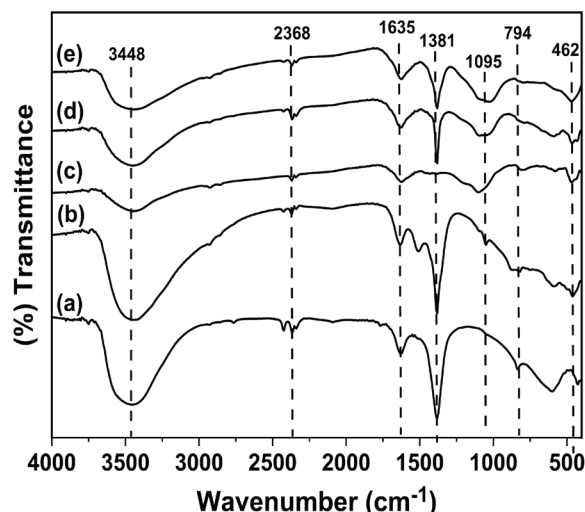


**Figure 2.** FTIR spectrum of Zn/Al LDH (a), Cu/Al LDH (b), BC (c), Zn/Al-BC (d), Cu/Al-BC (e)

which affected by the large increasing surface area of Zn/Al-BC than Cu/Al-BC. The surface area of Zn/Al LDH was smaller than Cu/Al LDH due to the formation of metal oxide, as previously mentioned on the XRD results.

The thermal analysis of materials was shown in (Fig.4). LDH consists of inorganic components; thus, the thermogravimetry patterns had only exothermic phase [Magri et al, 2019]. Exothermic peak of both Zn/Al and Cu/Al LDH was attributed to the decomposition of water at around 100-110°C, loss of anion on interlayer at around 200-300°C and decomposition of layer at around 650°C. On the other hand, BC had organic content; thus, the endothermic peak was found due to the oxidation of organic moiety at around 490°C. The composites had inorganic and organic components; thus, they had two kinds peaks i.e. exothermic and endothermic peaks, as shown in Figures 4d and e for Zn/Al-BC and Cu/Al-BC.

The performance of composites of Zn/Al-BC, Cu/Al-BC, and starting materials were evaluated by reusability and regeneration process toward re-adsorption of Cr(VI) as shown in (Fig. 5).

In proportion to the increase in surface area, the performance of the composite material was better in the five reusability cycles. The adsorption of Cr(VI) on composite was higher than that of the starting materials. The results of reusability of composites toward re-adsorption of Cr(VI) showed that Cu/Al-BC had higher structural stability than Zn/Al-BC. The adsorption of Cr(VI) on Cu/Al-BC was still greater than 60% after being used five times as adsorbent for Cr(VI). On

**Table 1.** Physical properties of composites and pristine LDH

| Materials | Surface area (m <sup>2</sup> /g) | Pore Size (nm), BJH | Pore Volume (cm <sup>3</sup> /g) <sub>BJH</sub> |
|-----------|----------------------------------|---------------------|---|
| Zn/Al LDH | 9.621                            | 12.094              | 0.017   |
| Cu/Al LDH | 46.279                           | 10.393              | 0.117   |
| BC        | 50.936                           | 12.089              | 0.025   |
| Zn/Al-BC  | 56.461                           | 12.226              | 0.065   |
| CuAl-BC   | 200.909                          | 7.032               | 0.324   |

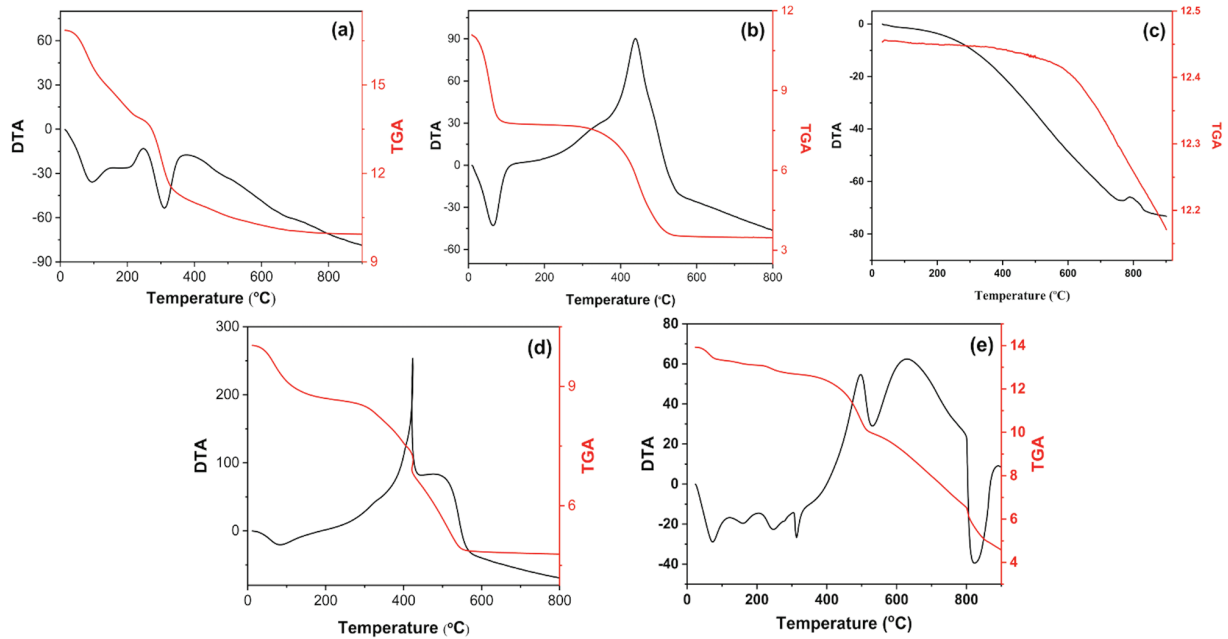


**Figure 4.** Thermogravimetric patterns of Zn/Al LDH (a), Cu/Al LDH (b), BC (c), Zn/Al-BC (d), Cu/Al-BC (e)

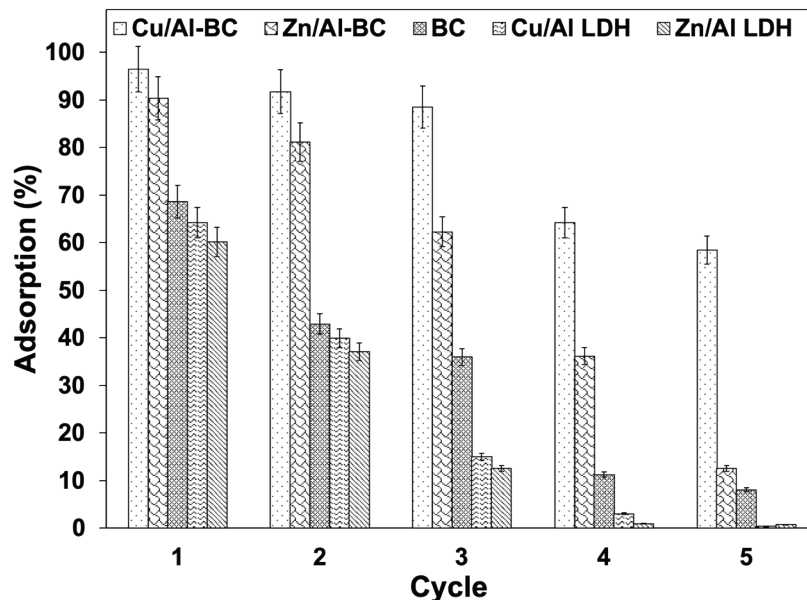


**Figure 5.** Reusability of composite and starting materials for adsorption of Cr(VI)

the other hand, the reusability of Zn/Al-BC was stable until three times cycles with more than 60% adsorption ability. The adsorption of Cr(VI)

was drastically decreased after four cycles adsorption by Zn/Al-BC. Thus, the structural stability of Cu/Al-BC was higher than Zn/Al-BC. On

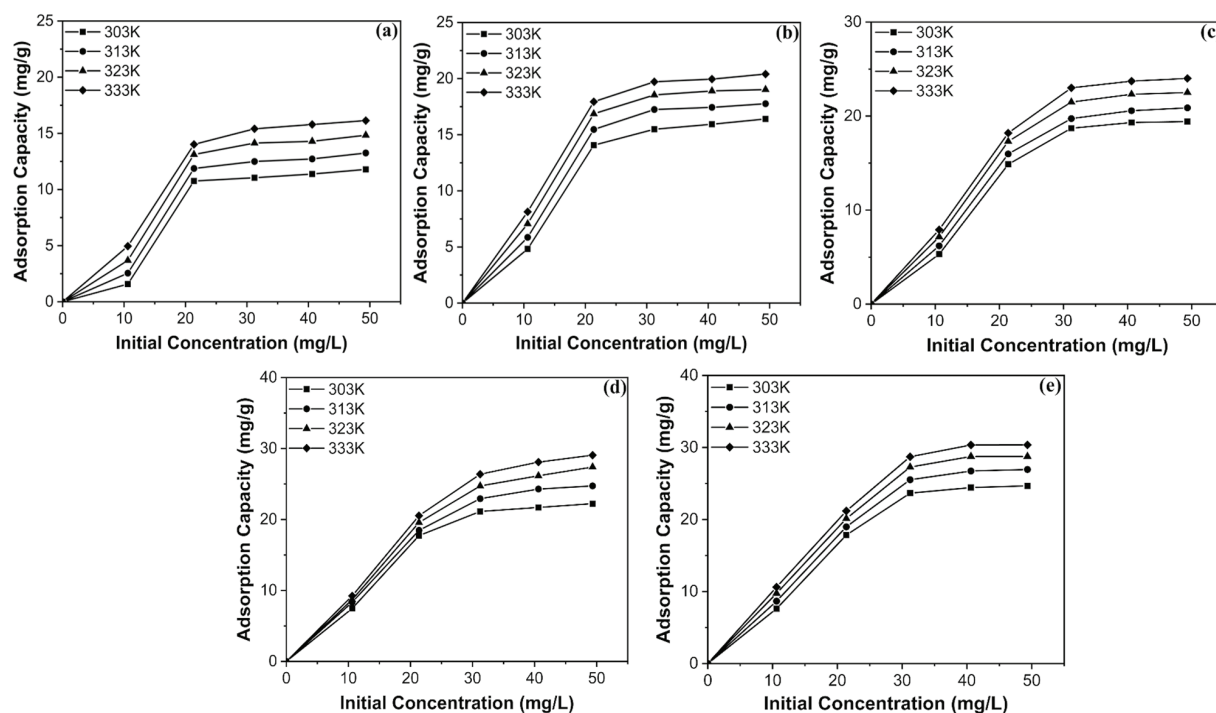


Figure 6. Effect of Cr(VI) initial concentration and adsorption temperature on composites and starting materials

Table 2. Isotherm of Cr(VI) on composites and starting materials

| Adsorbent | Adsorption Isotherm | Adsorption Constant | T (K)  |         |         |         |
|-----------|---------------------|---------------------|--------|---------|---------|---------|
|           |                     |                     | 303    | 313     | 323     | 333     |
| Zn/Al LDH | Langmuir            | Qmax                | 12.240 | 13.755  | 15.361  | 22.727  |
|           |                     | kL                  | 0.552  | 0.574   | 0.654   | 0.088   |
|           |                     | R <sup>2</sup>      | 0.998  | 0.998   | 0.999   | 0.999   |
|           | Freundlich          | n                   | 9.681  | 12.970  | 12.346  | 16.234  |
|           |                     | kF                  | 8.078  | 9.963   | 11.097  | 12.990  |
|           |                     | R <sup>2</sup>      | 0.976  | 0.964   | 0.960   | 0.992   |
| Cu/Al LDH | Langmuir            | Qmax                | 22.923 | 22.676  | 22.026  | 22.272  |
|           |                     | kL                  | 0.423  | 0.788   | 1.343   | 1.554   |
|           |                     | R <sup>2</sup>      | 0.999  | 0.999   | 0.999   | 0.999   |
|           | Freundlich          | n                   | 9.901  | 28.736  | 33.784  | 28.249  |
|           |                     | kF                  | 11.569 | 15.707  | 17.219  | 18.047  |
|           |                     | R <sup>2</sup>      | 0.982  | 0.921   | 0.979   | 0.899   |
| Zn/Al-BC  | Langmuir            | Qmax                | 46.668 | 243.902 | 500.000 | 666.667 |
|           |                     | kL                  | 0.504  | 0.038   | 0.024   | 0.030   |
|           |                     | R <sup>2</sup>      | 0.999  | 0.999   | 0.999   | 0.999   |
|           | Freundlich          | n                   | 8.889  | 14.124  | 12.180  | 14.859  |
|           |                     | kF                  | 15.635 | 19.797  | 21.164  | 23.719  |
|           |                     | R <sup>2</sup>      | 0.922  | 0.978   | 0.984   | 0.999   |
| Cu/Al-BC  | Langmuir            | Qmax                | 30.303 | 61.728  | 92.593  | 384.615 |
|           |                     | kL                  | 0.713  | 0.529   | 3.000   | 0.179   |
|           |                     | R <sup>2</sup>      | 0.998  | 0.970   | 0.999   | 0.999   |
|           | Freundlich          | n                   | 27.548 | 24.213  | 33.557  | 29.155  |
|           |                     | kF                  | 22.014 | 23.812  | 28.016  | 26.122  |
|           |                     | R <sup>2</sup>      | 0.982  | 0.955   | 0.915   | 0.894   |

the other hand, the starting materials of LDH can be effective as reuse adsorbent until two cycles adsorption. BC was an unstable structure toward the ultrasonic process; thus, the adsorption of Cr(VI) was sharply decreased at each cycle. Furthermore, the effect of initial concentration and adsorption temperature on the adsorption of Cr(VI) was studied as shown in (Fig. 6).

Adsorption of Cr(VI) on all adsorbents had sharply increased along with the initial concentration and reached equilibrium at almost 30 mg/L. Adsorption was also increased along with temperature from 303 to 333 K. Only one step adsorption was found for all adsorbents probably due to monolayer process of Cr(VI) on all adsorbents. The data in Figure 6 was then used to obtain the isotherm and thermodynamic properties.

The adsorption of Cr(VI) on composites and starting materials was firstly evaluated by adsorption isotherm, as shown in Table 2. The Langmuir and Freundlich isotherm models were applied to study the adsorption properties.

The composites Zn/Al-BC, Cu/Al-BC, pristine LDH, and BC more closely followed the Langmuir isotherm model than the Freundlich model for all temperatures. The  $R^2$  value was relative closer to the one for the Langmuir than

the Freundlich models [Gupta and Balomajumder, 2016]adsorbent dose, and contact time onto the percentage removal of both Cr(VI). The  $Q_{max}$  value was achieved at almost 333 K, except for BC at 303 K, as a result of unstable organic adsorbent at high temperature. The increasing  $Q_{max}$  value of pristine LDHs to composites was twenty nine-fold for Zn/Al-BC and sixteen-fold for Cu/Al-BC. The largely increased  $Q_{max}$  value of composites in comparison pristine LDHs did not equal to the increasing surface area properties [Palapa et al., 2020b]. As a result of the monolayer adsorption process, the chemisorption probably occurred on Cr(VI) with not only by the involvement of pore and layer of composite but also the functional groups of composite from BC [Jang et al., 2018]. Thus, the inorganic and organic components on the composite played a role to determine the high adsorption capacity of Cr(VI). As presented in Table 3, the composites of Zn/Al-BC and Cu/Al-BC had the highest adsorption capacity among other adsorbents given on the table. Thus, the composites Zn/Al-BC and Cu/Al-BC were potential adsorbents to remove Cr(VI) from aqueous solution.

Secondly, the thermodynamic adsorption of Cr(VI) was presented in (Table 4). The adsorption

**Table 3.** Adsorption of Cr(VI) by various adsorbents

| Adsorbent   | Adsorption capacity (mg/g) | Reference                    |
|---|----------------------------|------------------------------|
| Ni/Al@PAB   | 271.5                      | [Chen et al., 2018]          |
| Sand/MgAl-LDHs  | 29.401                     | [Gao et al., 2018]           |
| Sand/MgFe-LDHs  | 22.936                     | [Gao et al., 2018]           |
| Expanded graphite/Mg-Al LDH   | 13.44                      | [Hu et al., 2019]            |
| Core-shell maifanite/Zn-Al LDH                                      | 3.01                       | [Gao et al., 2020]           |
| Biochar with Mg/Al LDH Intercalated with EDTA                       | 38                         | [Huang et al., 2019]         |
| Ni/Mg/Al LDHs   | 103.4                      | [Lei et al., 2017]           |
| Magnetic litchi shell   | 58.769                     | [Li et al., 2020]            |
| CoFe-LDHs   | 27.62                      | [Ling et al., 2016]          |
| Fe@Mg/Al-Reduced graphene oxide                                     | 14.68                      | [Lv et al., 2019]            |
| Activated clay biochar composite                                    | 6.1                        | [Qhubu et al., 2021]         |
| Activated carbon  | 3.46                       | [Selvi et al., 2001]         |
| Fe <sub>3</sub> O <sub>4</sub> -ZnAl-LDH/TiO <sub>2</sub> composite | 44.76                      | [Yang et al., 2020]          |
| Surfactant-modified bentonite                                       | 9.61                       | [Castro-Castro et al., 2020] |
| Zn-Al-CO <sub>3</sub> LDHs  | 86.3                       | [Cochechi et al., 2010]      |
| Mg/Al LDH   | 12.56                      | [Otgonjargal et al., 2017]   |
| Mg/Zn-Al Hydrotalcites  | 25.80                      | [Cochechi et al., 2010]      |
| Ni/Fe LDHs  | 50.43                      | [Abo El-Reesh et al., 2020]  |
| Zn/Al LDH   | 22.727                     | This research                |
| Cu/Al LDH   | 22.923                     | This research                |
| BC  | 30.211                     | This research                |
| Zn/Al-BC  | 666.667                    | This research                |
| Cu/Al-BC  | 384.615                    | This research                |

**Table 4.** Thermodynamic adsorption of Cr(VI) on composites, pristine LDHs and BC.

| Materials | T (K) | $Q_e$ (mg/g) | $\Delta H$ (kJ/mol) | $\Delta S$ (kJ/mol.K) | $\Delta G$ (kJ/mol) |
|-----------|-------|--------------|---------------------|-----------------------|---------------------|
| Zn/Al LDH | 303   | 10.757       | 17.893              | 0.059                 | -0.022              |
|           | 313   | 11.871       |                     |                       | -0.614              |
|           | 323   | 13.119       |                     |                       | -1.205              |
|           | 333   | 14.013       |                     |                       | -1.796              |
| Cu/Al LDH | 303   | 14.062       | 27.049              | 0.095                 | -1.617              |
|           | 313   | 15.465       |                     |                       | -2.563              |
|           | 323   | 16.867       |                     |                       | -3.509              |
|           | 333   | 17.936       |                     |                       | -4.455              |
| BC        | 303   | 14.867       | 26.125              | 0.093                 | -2.011              |
|           | 313   | 15.973       |                     |                       | -2.940              |
|           | 323   | 17.306       |                     |                       | -3.868              |
|           | 333   | 18.196       |                     |                       | -4.797              |
| Zn/Al-BC  | 303   | 17.729       | 44.738              | 0.160                 | -3.619              |
|           | 313   | 18.481       |                     |                       | -5.215              |
|           | 323   | 19.578       |                     |                       | -6.811              |
|           | 333   | 20.534       |                     |                       | -8.407              |
| Cu/Al-BC  | 303   | 17.851       | 47.116              | 0.169                 | -3.967              |
|           | 313   | 18.989       |                     |                       | -5.653              |
|           | 323   | 20.131       |                     |                       | -7.339              |
|           | 333   | 21.188       |                     |                       | -9.025              |

energy was increased after the formation of composites reaching 44.738-47.116 kJ/mol. There were at least two contributions of the increasing adsorption energy on the composites. Firstly, the involvement of two active sites for Cr(VI) adsorption i.e. pores and functional groups. Secondly, the monolayer adsorption process created one by one adsorbent-adsorbate interaction [Mohamed et al., 2019], which increased the adsorption energy of Cr(VI). The  $\Delta G$  had negative values, which indicated that the adsorption of Cr(VI) on all materials was spontaneous [Ebelegi et al., 2020]. The value of  $\Delta G$  was more negative with increasing temperature. The  $\Delta S$  value was small and in the range 0.059-0.169 kJ/mol.K. The randomness was increased from the starting materials to composites as a result of two components involved in the adsorption [Palapa et al., 2020b; Taher et al., 2019].

## CONCLUSIONS

Formation of composites based on carbon material, i.e Zn/Al-BC and Cu/Al-BC, was successfully carried out. The surface area properties of Zn/Al-BC and Cu/Al-BC were six and four-fold greater than that of pristine LDHs. The

composite of Cu/Al-BC had high structural stability toward the reusability process until five cycles Cr(VI) re-adsorption process. The adsorption capacity of composites was higher than that of starting materials and amounted up to 384.615 mg/g for Cu/Al-BC and 666.667 mg/g for Zn/Al-BC. Thus, the composites of Cu/Al-BC and Zn/Al-BC can be used as a potential adsorbents to remove Cr(VI) from aqueous solutions.

## Acknowledgement

Authors greatly appreciated Universitas Sriwijaya for supporting this research by Hibah Profesi 2020-2021 contract number 0687/UN9/SK.BUK.KP/2020. Special thanks to Research Center of Inorganic Materials and Complexes FMIPA Universitas Sriwijaya for instrumental analysis.

## REFERENCES

1. Abo El-Reesh, G.Y., Farghali, A.A., Taha, M. and Mahmoud, R.K. 2020. Novel synthesis of Ni/Fe layered double hydroxides using urea and glycerol and their enhanced adsorption behavior for Cr(VI) removal. *Scientific Reports*, 10(1), 1–20.

2. Ali, I., Asim, M. and Khan, T.A. 2012. Low cost adsorbents for the removal of organic pollutants from wastewater. *Journal of Environmental Management*, 113, 170–183.
3. Altun, T. and Kar, Y. 2016. Removal of Cr(VI) from aqueous solution by pyrolytic charcoals. *Xinxing Tan Cailiao/New Carbon Materials*, 31, (5), 501–509.
4. Amen, R., Yaseen, M., Mukhtar, A., Klemeš, J.J., Saqib, S., Ullah, S., Al-Sehemi, A.G., Rafiq, S., Babar, M., Fatt, C.L., Ibrahim, M., Asif, S., Qureshi, K.S., Akbar, M.M. and Bokhari, A. 2020. Lead and cadmium removal from wastewater using eco-friendly biochar adsorbent derived from rice husk, wheat straw, and corncob. *Cleaner Engineering and Technology*, 100006.
5. Begum, T., Hoq, M.I., Mahmud, J., Pramanaik, M.K., Kamal, M.A.H.M., Islam, M.N. and Khan, R.A. 2019. Biodegradation of Hexavalent Chromium from Paint Industry Effluent by Indigenous Bacteria. *The Journal of Social Sciences Research*, 52, 45–52.
6. de Bittencourt, M.A., Novack, A.M., Scherer Filho, J.A., Mazur, L.P., Marinho, B.A., da Silva, A., de Souza, A.A.U. and de Souza, S.M.A.G.U. 2020. Application of FeCl<sub>3</sub> and TiO<sub>2</sub>-coated algae as innovative biophotocatalysts for Cr(VI) removal from aqueous solution: A process intensification strategy. *Journal of Cleaner Production*, 268(6), 122164.
7. Bouteraa, S., Boukraa, F., Saiah, D., Hamouda, S. and Bettahar, N. 2020. Zn-M-CO<sub>3</sub> Layered Double Hydroxides (M = Fe, Cr, or Al): Synthesis, Characterization, and Removal of Aqueous Indigo Carmine. 15(1), 43–54.
8. Castro-Castro, J.D., Macías-Quiroga, I.F., Giraldo-Gómez, G.I. and Sanabria-González, N.R. 2020. Adsorption of Cr(VI) in Aqueous Solution Using a Surfactant-Modified Bentonite. *Scientific World Journal*, 17.
9. Chen, S., Huang, Y., Han, X., Wu, Z., Lai, C., Wang, J., Deng, Q., Zeng, Z. and Deng, S. 2018. Simultaneous and efficient removal of Cr(VI) and methyl orange on LDHs decorated porous carbons. *Chemical Engineering Journal*, 352(VI), 306–315.
10. Cochechi, L., Barvinschi, P., Pode, R., Seftel, E.M. and Popovici, E. 2010. Chromium(VI) ion removal from aqueous solutions using a Zn-Al-type layered double hydroxide. *Adsorption Science and Technology*, 28(3), 267–279.
11. Ebelegi, A.N., Ayawei, N. and Wankasi, D. 2020. Interpretation of Adsorption Thermodynamics and Kinetics. *Open Journal of Physical Chemistry*, 10(3), 166–182.
12. Forghani, M., Azizi, A., Livani, M.J. and Kafshgari, L.A. 2020. Adsorption of lead(II) and chromium(VI) from aqueous environment onto metal-organic framework MIL-100(Fe): Synthesis, kinetics, equilibrium and thermodynamics. *Journal of Solid State Chemistry*, 291, 121636.
13. Gao, J., Zhang, X., Yu, J., Lei, Y., Zhao, S., Jiang, Y., Xu, Z. and Cheng, J. 2020. Cr(VI) removal performance and the characteristics of microbial communities influenced by the core-shell maifanite/ZnAl-layered double hydroxides (LDHs) substrates for chromium-containing surface water. *Biochemical Engineering Journal*, 160, 107625.
14. Gao, C., Zhang, X., Yuan, Y., Lei, Y., Gao, J., Zhao, S., He, C. and Deng, L. 2018. Removal of hexavalent chromium ions by core-shell sand/Mg-layer double hydroxides (LDHs) in constructed rapid infiltration system. *Ecotoxicology and Environmental Safety*, 166, 285–293.
15. Gasemloo, S., Khosravi, M., Sohrabi, M.R., Dastmalchi, S. and Gharbani, P. 2019. Response surface methodology (RSM) modeling to improve removal of Cr(VI) ions from tannery wastewater using sulfated carboxymethyl cellulose nanofilter. *Journal of Cleaner Production*, 208(6), 736–742.
16. Golder, A.K., Chanda, A.K., Samanta, A.N. and Ray, S. 2007. Removal of Cr(VI) from aqueous solution: Electrocoagulation vs chemical coagulation. *Separation Science and Technology*, 42(10), 2177–2193.
17. Gupta, A. and Balomajumder, C. 2016. Simultaneous adsorption of Cr(VI) and phenol from binary mixture using iron incorporated rice husk: Insight to multicomponent equilibrium isotherm. *International Journal of Chemical Engineering*, 6, 1-11.
18. Hosseinkhani, A., Forouzes Rad, B. and Baghdadi, M. 2020. Efficient removal of hexavalent chromium from electroplating wastewater using polypyrrole coated on cellulose sulfate fibers. *Journal of Environmental Management*, 274, 111153.
19. Hu, Z., Cai, L., Liang, J., Guo, X., Li, W. and Huang, Z. 2019. Green synthesis of expanded graphite/layered double hydroxides nanocomposites and their application in adsorption removal of Cr(VI) from aqueous solution. *Journal of Cleaner Production*, 209(6), 1216–1227.
20. Huang, D., Liu, C., Zhang, C., Deng, R., Wang, R., Xue, W., Luo, H., Zeng, G., Zhang, Q. and Guo, X. 2019. Cr(VI) removal from aqueous solution using biochar modified with Mg/Al-layered double hydroxide intercalated with ethylenediaminetetraacetic acid. *Bioresource Technology*, 276, 127–132.
21. Itankar, N. and Patil, Y. 2014. Management of Hexavalent Chromium from Industrial Waste Using Low-cost Waste Biomass. *Procedia - Social and Behavioral Sciences*, 133, 219–224.
22. Jang, H.M., Yoo, S., Choi, Y.K., Park, S. and Kan, E. 2018. Adsorption isotherm, kinetic modeling and mechanism of tetracycline on Pinus taeda-derived activated biochar. *Bioresource Technology*, 259, 24–31.
23. Kahlon, S.K., Sharma, G., Julka, J.M., Kumar, A.,

- Sharma, S. and Stadler, F.J. 2018. Impact of heavy metals and nanoparticles on aquatic biota. *Environmental Chemistry Letters*, 16(3), 919–946.
24. Kaur, J., Kaur, M., Ubhi, M.K., Kaur, N. and Greneche, J.M. 2021. Composition optimization of activated carbon-iron oxide nanocomposite for effective removal of Cr(VI) ions. *Materials Chemistry and Physics*, 258, 124002.
25. Kaykhah, M., Sasani, M. and Marghzari, S. 2018. Removal of Dyes from the Environment by Adsorption Process. *Chemical and Materials Engineering*, 6(2), 31–35.
26. Lei, C., Zhu, X., Zhu, B., Jiang, C., Le, Y. and Yu, J. 2017. Superb adsorption capacity of hierarchical calcined Ni/Mg/Al layered double hydroxides for Congo red and Cr(VI) ions. *Elsevier B.V.*, 801–811.
27. Li, L., Cao, G. and Zhu, R. 2020. Adsorption of Cr(VI) from aqueous solution by a litchi shell-based adsorbent. *Environmental Research*, VI, 110356.
28. Ling, F., Fang, L., Lu, Y., Gao, J., Wu, F., Zhou, M. and Hu, B. 2016. A novel CoFe layered double hydroxides adsorbent: High adsorption amount for methyl orange dye and fast removal of Cr(VI). *Microporous and Mesoporous Materials*, 234(VI), 230–238.
29. Lv, X., Qin, X., Wang, K., Peng, Y., Wang, P. and Jiang, G. 2019. Nanoscale zero valent iron supported on MgAl-LDH-decorated reduced graphene oxide: Enhanced performance in Cr(VI) removal, mechanism and regeneration. *Journal of Hazardous Materials*, 373, 176–186.
30. Magri, V.R., Duarte, A., Perotti, G.F. and Constantino, V.R.L. 2019. Investigation of thermal behavior of layered double hydroxides intercalated with carboxymethylcellulose aiming bio-carbon based nanocomposites. *ChemEngineering*, 3(2), 1–17.
31. Mandal, S., Tripathy, S., Padhi, T., Sahu, M.K. and Patel, R.K. 2013. Removal efficiency of fluoride by novel Mg-Cr-Cl layered double hydroxide by batch process from water. *Journal of Environmental Sciences (China)*, 25, (5), 993–1000.
32. Marques, B.S., Dalmagro, K., Moreira, K.S., Oliveira, M.L.S., Jahn, S.L., de Lima Burgo, T.A. and Dotto, G.L. 2020. Ca-Al, Ni-Al and Zn-Al LDH powders as efficient materials to treat synthetic effluents containing o-nitrophenol. *Journal of Alloys and Compounds*, 838.
33. Miguel, G.S., Lambert, S.D. and Graham, N.J. 2008. Wastewater treatment for production of H<sub>2</sub>S-free biogas. *Journal of Chemical Technology & Biotechnology*, 83, 1163–1169.
34. Mir, Z.M., Bastos, A., Höche, D. and Zheludkevich, M.L. 2020. Recent advances on the application of layered double hydroxides in concrete-A review. *Materials*, 13(6), 1–23.
35. Mohamed, E., Kamal, E., Doha, B., Samira, S. and Abdessalem, T. 2019. Adsorption thermodynamics and isosteric heat of adsorption of Thymol onto sodic, pillared and organic bentonite. *Mediterranean Journal of Chemistry*, 8(6), 494–504.
36. Moller, M. and Pich, A. Development of Modified Layered Silicates with Superior Adsorption Properties for Uptake of Pollutants from Air and Water.
37. Naggar, Y.I., Khalil, M.S. and Ghorab, M.A. 2018. Environmental Pollution by Heavy Metals in the Aquatic Ecosystems of Egypt. *Open Access Journal of Toxicology*, 3(1).
38. Oktriyanti, M., Palapa, N.R., Mohadi, R. and Lesbani, A. 2019. Modification Of Zn-Cr Layered Double Hydroxide With Keggin Ion as Cr(VI) Adsorbent. *Indonesian Journal of Environmental Management and Sustainability*, 3(3), 93–99.
39. Otgonjargal, E., Nyamsuren, B., Surenjav, E., Burmaa, G., Temuujin, J. and Dashkhuu, K. 2017. Removal of Chromium from Aqueous Solution by Thermally Treated MgAl Layered Double Hydroxide. *Annals of Civil and Environmental Engineering*, 1(1), 1–8.
40. Palapa, N.R., Juleanti, N., Normah, N., Taher, T. and Lesbani, A. 2020a. Unique Adsorption Properties of Malachite Green on Interlayer Space of Cu-Al and Cu-Al-SiW 12 O 40 Layered Double Hydroxides. *Bulletin of Chemical Reaction Engineering & Catalysis*. 15(3), 653–661.
41. Palapa, N.R., Saria, Y., Taher, T., Mohadi, R. and Lesbani, A. 2019. Synthesis and Characterization of Zn/Al, Zn/Fe, and Zn/Cr Layered Double Hydroxides: Effect of M<sup>3+</sup> ions Toward Layer Formation. *Science and Technology Indonesia*, 4(2), 36–39.
42. Palapa, N.R., Taher, T., Rahayu, B.R., Mohadi, R., Rachmat, A. and Lesbani, A. 2020b. CuAl LDH/ Rice Husk Biochar Composite for Enhanced Adsorptive Removal of Cationic Dye from Aqueous Solution. *Bulletin of Chemical Reaction Engineering & Catalysis*, 15(2), 525–537.
43. Qhubu, M.C., Mgidlana, L.G., Madikizela, L.M. and Pakade, V.E. 2021. Preparation, characterization and application of activated clay biochar composite for removal of Cr (VI) in water: Isotherms, kinetics and thermodynamics. *Materials Chemistry and Physics*, 260, 124165.
44. Rahman, Z. 2020. An overview on heavy metal resistant microorganisms for simultaneous treatment of multiple chemical pollutants at co-contaminated sites, and their multipurpose application. *Journal of Hazardous Materials*, 396, 122682.
45. Saha, R., Nandi, R. and Saha, B. 2011. Sources and toxicity of hexavalent chromium. *Journal of Coordination Chemistry*, 64(10), 1782–1806.
46. Selvi, K., Pattabhi, S. and Kadirvelu, K. 2001. Removal of Cr(VI) from aqueous solution by adsorption onto activated carbon. *Bioresource Technology*, 80(1), 87–89.

47. Semeraro, P., Fini, P., D'Addabbo, M., Rizzi, V. and Cosma, P. 2017. Removal from wastewater and recycling of azo textile dyes by alginate-chitosan beads. *International Journal of Environment, Agriculture and Biotechnology*, 2(4), 1835–1850.
48. Shan, R. ran, Yan, L. guo, Yang, Y. ming, Yang, K., Yu, S. jun, Yu, H. qin, Zhu, B. cun and Du, B. 2015. Highly efficient removal of three red dyes by adsorption onto Mg-Al-layered double hydroxide. *Journal of Industrial and Engineering Chemistry*, 21, 561–568.
49. Silaen, L., Palapa, N.R., Juleanti, N., Mohadi, R. and Lesbani, A. 2020. Efficient Adsorption of Cadmium (II) on Zn/M<sup>3+</sup> (M<sup>3+</sup> = Al, Cr). *ARPN Journal*, 15(18), 1967–1975.
50. Sivamani, S. and Leena, G.B. 2009. Removal of Dyes from Wastewater using Adsorption - A Review. *International Journal of BioSciences and Technology*, 2(4), 47–51.
51. Sun, D., Zhang, Z., Wang, M. and Wu, Y. 2013. Adsorption of Reactive Dyes on Activated Carbon Developed from *Enteromorpha prolifera*. *American Journal of Analytical Chemistry*, 4(7), 17–26.
52. Taher, T., Rohendi, D., Mohadi, R. and Lesbani, A. 2019. Congo red dye removal from aqueous solution by acid-activated bentonite from sarolangun: kinetic, equilibrium, and thermodynamic studies. *Arab Journal of Basic and Applied Sciences*, 26(1), 125–136.
53. Vieira, F.R., Romero Luna, C.M., Arce, G.L.A.F. and Ávila, I. 2020. Optimization of slow pyrolysis process parameters using a fixed bed reactor for biochar yield from rice husk. *Biomass and Bioenergy*, 132.
54. Wang, X., Liu, X., Xiao, C., Zhao, H., Zhang, M., Zheng, N., Kong, W., Zhang, L., Yuan, H., Zhang, L. and Lu, J. 2020. Triethylenetetramine-modified hollow Fe<sub>3</sub>O<sub>4</sub>/SiO<sub>2</sub>/chitosan magnetic nanocomposites for removal of Cr(VI) ions with high adsorption capacity and rapid rate. *Microporous and Mesoporous Materials*, 297, 110041.
55. Wu, Y., Guan, C.Y., Griswold, N., Hou, L. yuan, Fang, X., Hu, A., Hu, Z. qiang and Yu, C.P. 2020. Zero-valent iron-based technologies for removal of heavy metal(loid)s and organic pollutants from the aquatic environment: Recent advances and perspectives. *Journal of Cleaner Production*, 277, 123478.
56. Yang, Y., Li, J., Yan, T., Zhu, R., Yan, L. and Pei, Z. 2020. Adsorption and photocatalytic reduction of aqueous Cr(VI) by Fe<sub>3</sub>O<sub>4</sub>-ZnAl-layered double hydroxide/TiO<sub>2</sub> composites. Elsevier Inc., 493–501.
57. Zhang, S., Lü, T., Mu, Y., Zheng, J. and Meng, C. 2020. High adsorption of Cd (II) by modification of synthetic zeolites Y, A and mordenite with thiourea. *Chinese Journal of Chemical Engineering*, (II).